Defect and Diffusion Forum Vol. 333 (2013) pp 39-49
Online available since 2013/Jan/25 at www.scientific.net

doi:10.4028/www.scientific.net/DDF.333.39

Anisotropy of Hydrogen Diffusivity in ZnO

Jakub Čížek[1,a], Fratišek Lukáč[1,b], Marián Vlček[1,c], Martin Vlach[1,d], Ivan Procházka[1,e], Franziska Traeger[2,f], Detlef Rogalla[2,g], Hans-Werner Becker [2,h], Wolfgang Anwand[3,i], Gerhard Brauer[3,j], Stefan Wagner[4,k], Helmut Uchida[4,l], Astrid Pundt[4,m], Carsten Bähtz[5,n]

[1]Faculty of Mathematics and Physics, Charles University, Holešovičkách 2, CZ-180 00 Praha 8, Czech Republic

[2]Physikalische Chemie I, Ruhr-Universitaet Bochum, Universitaetsstr. 150, D-44801 Bochum, Germany

[3]Institut für Strahlenphysik, Helmholtz-Zentrum Dresden-Rossendorf, PO Box 510 119, D-01314 Dresden, Germany

[4]Institute for Materials Physics, University of Göttingen, Friedrich-Hund-Platz 1, D-37077, Göttingen, Germany

[5]European Synchrotron Radiation Facility (ESRF), Polygone Scientique Louis Néel, 6 rue Jules Horowitz, 38000, Grenoble, France

[a]jakub.cizek@mff.cuni.cz, [b]frantisek.lukac@gmail.com, [c]vlko.majo@centrum.sk, [d]martin.vlach@mff.cuni.cz, [e]ivan.prochazka@mff.cuni.cz, [f]traeger@pc.rub.de, [g]rogalla@rubion.rub.de, [h]Hans-Werner.Becker@rub.de, [i]w.anwand@hzdr.de, [j]g.brauer@hzdr.de,' [k]swagner@ump.gwdg.de, [l]huchida@ ump.gwdg.de, [m]apundt@ump.gwdg.de, [n]sc.baehtz@hzdr.de

Keywords: zinc oxide, hydrogen, nuclear reaction analysis, electrical resistivity, X-ray diffraction.

Abstract. Hydrogen absorption and diffusivity in high quality ZnO crystals were investigated in this work by X-ray diffraction combined with slow positron implantation spectroscopy and electrical resistometry. ZnO crystals were covered by a thin Pd over-layer and electrochemically charged with hydrogen. It was found that absorbed hydrogen causes plastic deformation in a sub-surface region. The depth profile of hydrogen concentration introduced into the crystal was determined by nuclear reaction analysis. Enhanced hydrogen concentration was found in the sub-surface region due to excess hydrogen atoms trapped at defects introduced by plastic deformation. Hydrogen diffusion in ZnO crystals with various orientations was studied by *in-situ* electrical resistometry. It was found that hydrogen diffusion in the *c*-direction is faster than hydrogen diffusion in the *a*-direction most probably due to open channels existing in the wurtzite structure along the *c*-axis.

Introduction

ZnO is a wide band gap semiconductor with a large exciton binding energy. Because of its favorable properties ZnO has taken great attention as a material for UV light emitting diodes, optoelectronic devices, transparent electrodes for solar cells and gas sensors [1,2]. Due to progress in crystal growth, high quality ZnO single crystals are nowadays available [3]. Most ZnO crystals exhibit *n*-type conductivity likely due to some impurities or defects introduced unintentionally into ZnO lattice during the crystal growth [4]. On the other hand, acceptor doping leading stable *p*-type conductivity remains still an unsolved problem. Using *ab-inito* theoretical calculations Van de Walle [5] predicted that hydrogen is easily incorporated into ZnO lattice and can form a shallow donor state. Later experimental studies revealed that hydrogen is indeed the most important impurity in high quality ZnO crystals and its concentration exceeds the concentration of other impurities by at least one order of magnitude [6]. Moreover, recently it was shown that very high concentration of hydrogen can be introduced into ZnO by electrochemical charging [7]. For these reasons it is very important to understand hydrogen behavior in ZnO lattice.

In the present work, hydrogen-induced structural changes and hydrogen diffusivity in high quality ZnO single crystals electrochemically charged with hydrogen were investigated by slow positron implantation spectroscopy (SPIS) [8] combined with X-ray diffraction (XRD) and *in-situ* measurement of electrical resistivity. The depth profile of hydrogen concentration introduced into ZnO crystals was determined by nuclear reaction analysis (NRA) [9].

Experimental

Hydrothermally grown ZnO single crystals (MaTecK GmbH) with dimensions 10 x 10 x 0.5 mm^3 and O-terminated optically polished surfaces were investigated. Hydrogen diffusion in ZnO crystals with (0001) and (10-10) orientation were compared. The crystal faces (10 x 10 mm^2 area) were always covered by a 20 nm thick Pd cap deposited by a cold cathode beam sputtering. The Pd over-layer acts as a catalyst for dissociation of H_2 molecules on the surface and facilitates hydrogen permeation into ZnO [10]. The ZnO crystals were electrochemically doped with hydrogen using a Pt counter electrode and constant current pulses. Electrochemical hydrogen charging was performed at room temperature in a special cell filled with a 1:1 mixture of H_3PO_4 and glycerin. The hydrogen concentration c_H introduced into the sample can be estimated from the transported charge using the Faraday's law:

$$c_H = \frac{ItV_m}{FV}, \tag{1}$$

where I is the loading current, t is the duration of the loading pulse, V_m is the ZnO molar volume, V is the volume of the loaded sample and F is the Faraday's constant.

The hydrogen concentration introduced into the sample was determined by NRA using the resonant nuclear reaction $^{15}N + {}^{1}H \rightarrow {}^{12}C + {}^{4}He + \gamma$–rays [9]. NRA studies were performed by ^{15}N ions with energy adjustable in the range from 6.39 to 7.2 MeV. Penetration of ^{15}N ions into ZnO increases with increasing energy from the surface up to a depth of 300 nm. Hence using ^{15}N ions with adjustable energy depth profile of hydrogen concentration in the sample can be determined.

SPIS investigations were performed on a slow positron beam SPONSOR [11] with energy E of incident positrons adjustable in the range from 0.03 to 36 keV. Doppler broadening (DB) of annihilation photopeak was measured by a HPGe detector with an energy resolution of (1.09 ± 0.01) keV at 511 keV. Evaluation of DB was performed using the line shape S parameter. The central energy region for calculation of S was chosen as $|E - m_0c^2| < 0.93$ keV. All S parameters presented in this paper are normalized to the bulk value $S_0 = 0.5068(5)$ determined in the virgin ZnO crystal at the positron energy of 35 keV

Electrical resistivity of Pd over-layer was measured *in-situ* during hydrogen loading by DC four point method using a source meter Keithley 2400-C.

XRD studies were performed using synchrotron radiation with the wavelength of 1.078 Å. XRD measurements were carried out at the European Synchrotron Radiation Facility (ESRF) on the beamline BM20 equipped with a 4-axis Eulerian cradle.

Results and discussion

Figure 1(a) shows results of NRA characterization of ZnO (0001) crystals electrochemically loaded with hydrogen for 3 h using the current $I = 0.5$ mA. Two samples loaded with hydrogen in different arrangements were investigated and NRA investigations were performed on the loaded side covered with Pd cap and also on the opposite side without Pd cap. As shown schematically in Fig. 1(b) sample 1 was fully immersed in electrolyte during hydrogen charging, while sample 2 was loaded in the arrangement sketched in Fig. 1(c). Only the loaded side covered with Pd was deluged by electrolyte while the opposite side was in air without any contact with electrolyte. One can see in Fig. 1(a) that the hydrogen concentration profile measured on the loaded side (full points) is very similar for both samples. The hydrogen concentration c_H on the surface is very high testifying that the Pd over-layer was transformed into the hydride phase (PdH). The hydrogen concentration inside ZnO is very high as well. With increasing depth c_H readily decreases and its depth dependence can

be well described by an exponential decay function, see solid lines in Fig. 1(a). In the Pd over-layer c_H decreases faster than in the ZnO crystal. Therefore, the depth dependences of c_H in Pd cap and in ZnO crystal were fitted separately by exponential decay functions with different decay constants. A step in the depth dependence of hydrogen concentration can be observed at the interface between the Pd cap and the ZnO crystal at the depth of 20 nm, see Fig. 1(a). The hydrogen concentration at the interface is enhanced due to hydrogen trapped open volume misfit defects and the interface.

The depth dependence of hydrogen concentration measured on the opposite side of the sample 1 (open circles in Fig. 1(a)) differs significantly from that measured on the sample 2 (open triangles in Fig. 1(a)). The sample 1 which was fully immersed in electrolyte exhibits enhanced c_H in the sub-surface region also on the opposite side. This indicates that if the sample is completely immersed in the electrolyte, hydrogen is introduced into the crystal not only through the loaded side but also through the opposite side. This happens due to the relatively low resistivity of hydrothermally grown ZnO crystals which always exhibit *n*-type conductivity [4]. On the other hand, the sub-surface layer was not formed in the sample 2 loaded in the arrangement shown in Fig. 1(c), when the opposite side was not in contact with electrolyte. One can see in Fig. 1(a) that the sample 2 exhibits enhanced c_H only just on the surface due to weakly bound adsorbed hydrogen [12].

The total concentration of hydrogen introduced into the sample calculated from the transported charge by Eq. (1) is 4.2 at.% and is plotted in Fig. 1(a) by a dashed line. This value is in a reasonable agreement with c_H determined by NRA on the opposite side of the sample 2. From extrapolation of the exponential decay functions describing the depth profile of c_H in the sub-surface layers on the loaded side in samples 1, 2 and on the opposite side in sample 1 we obtained bulk hydrogen concentration of (4 ± 1) at.% which also agrees well with the value estimated from Faraday's law. Note that this concentration of hydrogen is more than two orders of magnitude higher than c_H = 0.03 at.% detected by NRA in the virgin crystal [12].

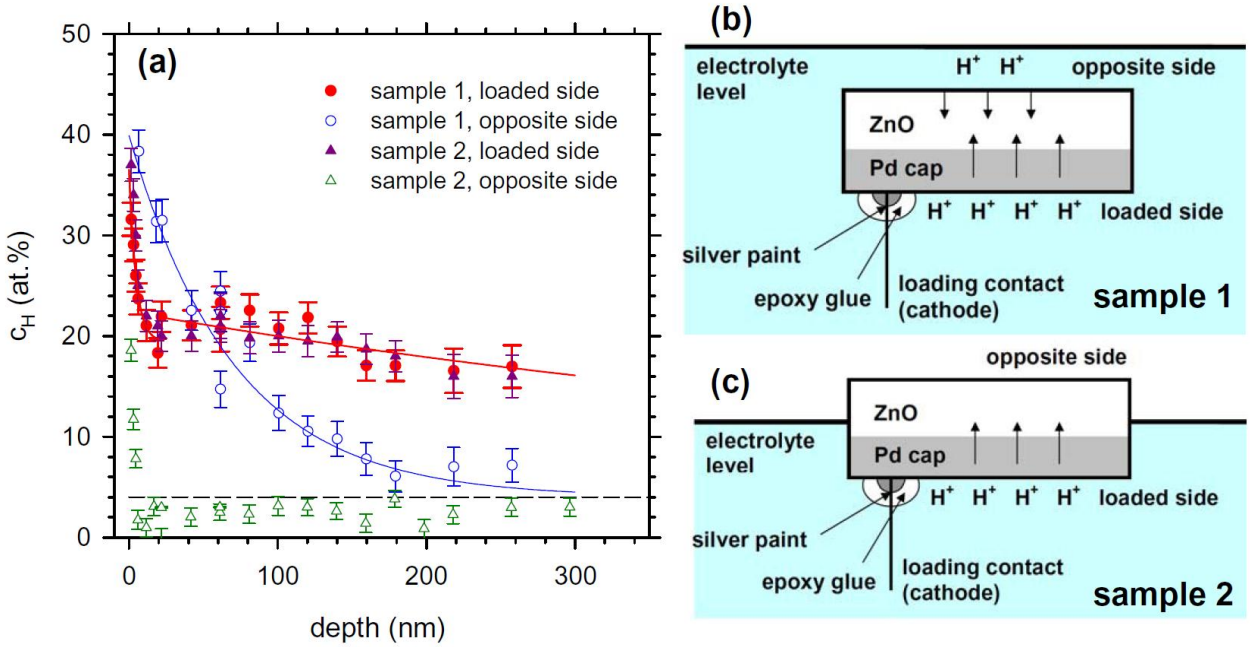

Figure 1 (a) Depth profile of hydrogen concentration determined by NRA in ZnO (0001) crystals loaded with hydrogen (t = 3 h, I = 0.5 mA) in two different arrangements: sample 1 was completely immersed in electrolyte (b), while sample 2 was deluged by electrolyte on the loaded side only and the opposite was in air without any contact with electrolyte (c).

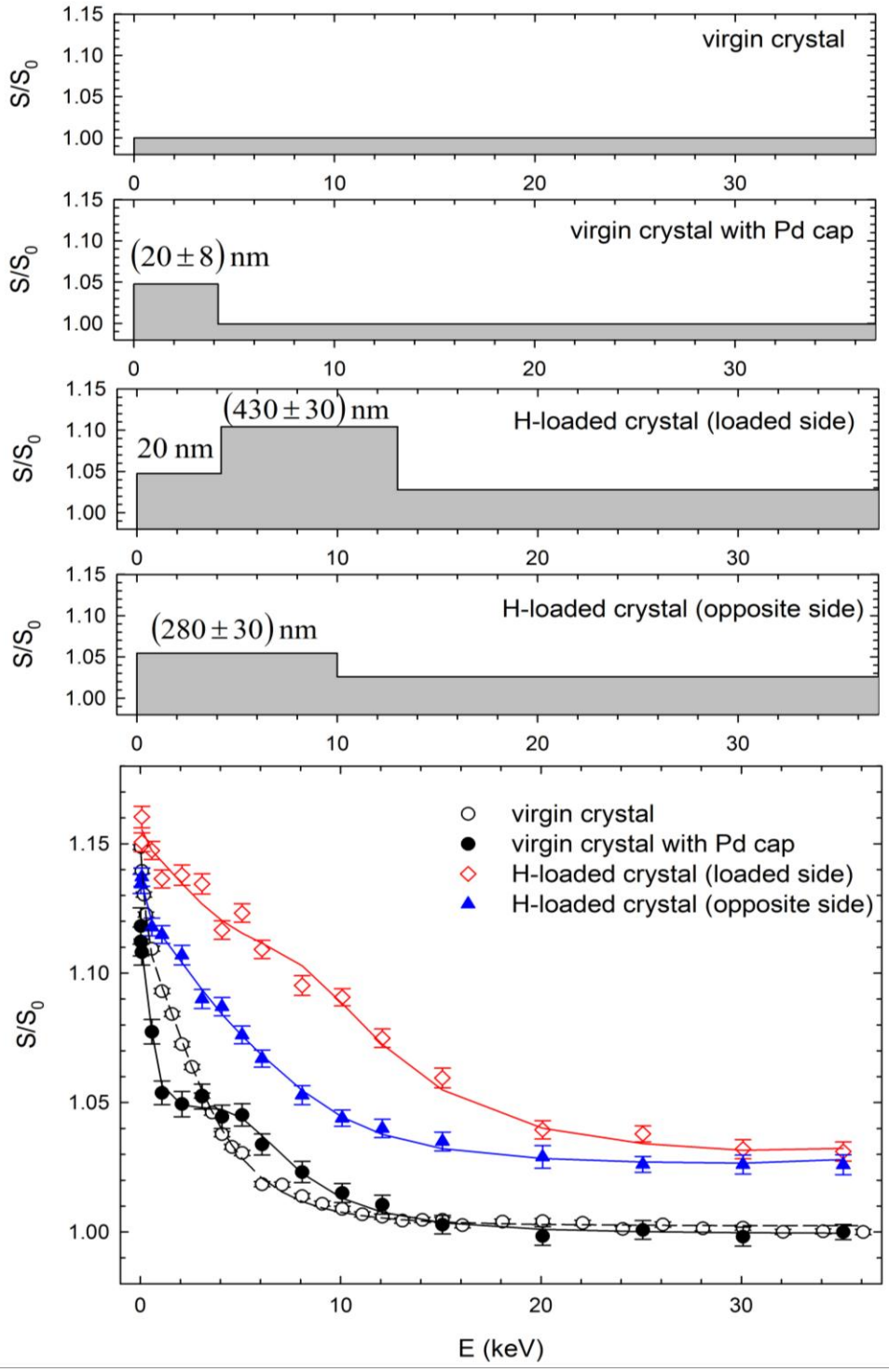

Figure 2 Dependence of the *S* parameter on positron energy *E* for the virgin ZnO (0001) crystal, the virgin crystal covered with Pd cap, and the hydrogen loaded crystal (t = 24 h, I = 0.3 mA) measured on the loaded and the opposite side. Solid lines show fit by model curve calculated by VEPFIT. Layer models used in fitting of various samples are shown in the upper panels. A single layer model was assumed for the virgin crystal, two layer model consisting of Pd cap and ZnO bulk was used for the virgin crystal covered with Pd cap. The *S(E)* curve of hydrogen-loaded crystal was fitted using three layer model consisting of Pd cap, defect-rich sub-surface layer and ZnO bulk, while the *S(E)* curve measured on the opposite side consisted of two layers: defect-rich sub-surface layer and ZnO bulk. Thicknesses of the layers obtained from fitting are shown in the upper panels. In order to reduce the number of free parameters in fitting of hydrogen-loaded crystal (loaded side) the thickness of Pd cap was fixed at the value of 20 nm determined previously on the virgin crystal.

The hydrogen concentration is substantially increased in the sub-surface region on the loaded side and also on the opposite side if the sample is fully immersed in electrolyte. To understand formation of the sub-surface region ZnO crystals were further characterized by SPIS.

Fig. 2 shows the dependence of the *S* parameter on the energy *E* of incident positrons for ZnO (0001) crystal. At very low energies virtually all positrons annihilate on the surface. With increasing energy positrons penetrate deeper and deeper into the crystal and the fraction of positrons diffusing back to the surface decreases which is reflected by a decrease of the *S* parameter from the surface value to the bulk value corresponding to the situation when all positrons annihilate inside ZnO crystal. The *S(E)* curve measured on the virgin crystal (open circles in Fig. 2) was fitted by a model curve calculated by VEPFIT [13] as a solution of positron diffusion-annihilation equation in a homogeneous single ZnO layer, see upper panel in Fig. 2. The model curve calculated by VEPFIT which is plotted in Fig. 2 by a dashed line describes the experimental points accurately. The positron diffusion length in the virgin ZnO crystal $L_+ = (58 \pm 2)$ nm obtained from fitting is in reasonable agreement with the positron diffusion length of 52 nm determined in a ZnO single crystal by Koida et al. [14], but is significantly shorter than the mean positron diffusion length of about 100-200 nm typical for nearly defect-free semiconductors [15]. This indicates that the virgin crystal contains positron traps. Indeed, investigations of the virgin crystal by means of positron lifetime spectroscopy combined with *ab-initio* theoretical calculations revealed saturated positron trapping in defects identified as Zn-vacancies associated with hydrogen impurities (V_{Zn+H} complexes) [6].

Deposition of Pd cap modifies the *S(E)* curve in the low energy region due to contribution of positrons annihilated in the Pd over-layer, see full circles in Fig. 2. However, at higher energies the *S(E)* curve remains virtually unchanged testifying that deposition of Pd over-layer introduced additional defects into the crystal. The *S(E)* curve for the virgin crystal covered by Pd cap was fitted by a model curve calculated for a two-layer model shown in the upper panel in Fig. 2 and consisting of (i) Pd cap and (ii) ZnO bulk. The model curve calculated by VEPFIT is plotted in Fig. 2 by a solid line. Again a good agreement of the model curve with experimental points has been achieved. The thickness of Pd-over layer obtained from fitting is (20 ± 8) nm and agrees well with the thickness estimated from the known sputtering rate and the time of deposition. The positron diffusion length of (50 ± 10) nm obtained from fitting for the virgin ZnO crystal covered with Pd cap is comparable with that for the virgin crystal measured prior to deposition of Pd cap.

The *S(E)* curves measured on the loaded side and on the opposite side of ZnO (0001) crystal loaded with hydrogen for the period $t = 24$ h using the current $I = 0.3$ mA are plotted in Fig. 2 by open diamonds and full triangles, respectively. The sample was fully immersed in electrolyte during hydrogen charging. One can see in Fig. 2 that hydrogen loading leads to a large increase of the *S* parameter in a sub-surface region corresponding to the positron energy range 1-14 keV. Hence, SPIS results testify that a sub-surface region with very high concentration of defects was formed by hydrogen loading. This strongly supports the picture of hydrogen-induced plastic deformation occurring in the sub-surface region and introducing a high density of open volume defects. The sub-surface region with high density of defects was found also on the opposite side (full triangles in Fig. 2). As shown schematically in the upper panels in Fig. 2 the *S(E)* curves of hydrogen loaded crystals were fitted by a model consisting (i) Pd cap (on the loaded side only) with thickness of 20 nm, (ii) sub-surface layer with very high concentration of defects and (iii) bulk ZnO layer. The model curves calculated by VEPFIT and plotted in Fig. 2 by solid lines are obviously in a good agreement with the experimental points. The thickness of defected sub-surface region obtained from fitting is (430 ± 30) nm and (280 ± 30) nm for the loaded and the opposite side, respectively. The positron diffusion length in the sub-surface region on the loaded side and on the opposite side is (20 ± 5) nm and (30 ± 8) nm, respectively. Hence, positron diffusion length in the sub-surface region is significantly shortened due to new defects introduced by hydrogen-induced plastic deformation. The defected sub-surface region on the loaded side is thicker and contains higher density of defects which is reflected by higher *S* parameter values and shorter positron diffusion length. Note that the thickness of the hydrogen-enriched defected layer on the loaded side of the sample is higher than

the maximum penetration depth of ^{15}N ions with energy of 7.2 MeV while on the opposite side it is comparable with it. Thus, NRA probes predominantly the sub-surface layers with high density of open volume defects acting as trapping sites for hydrogen atoms incoming from the electrolyte. This explains the enhanced hydrogen concentration in the sub-surface regions detected by NRA in samples 1,2 on the loaded side and in the sample 1 also on the opposite side exposed to the electrolyte, see Fig. 1(a).

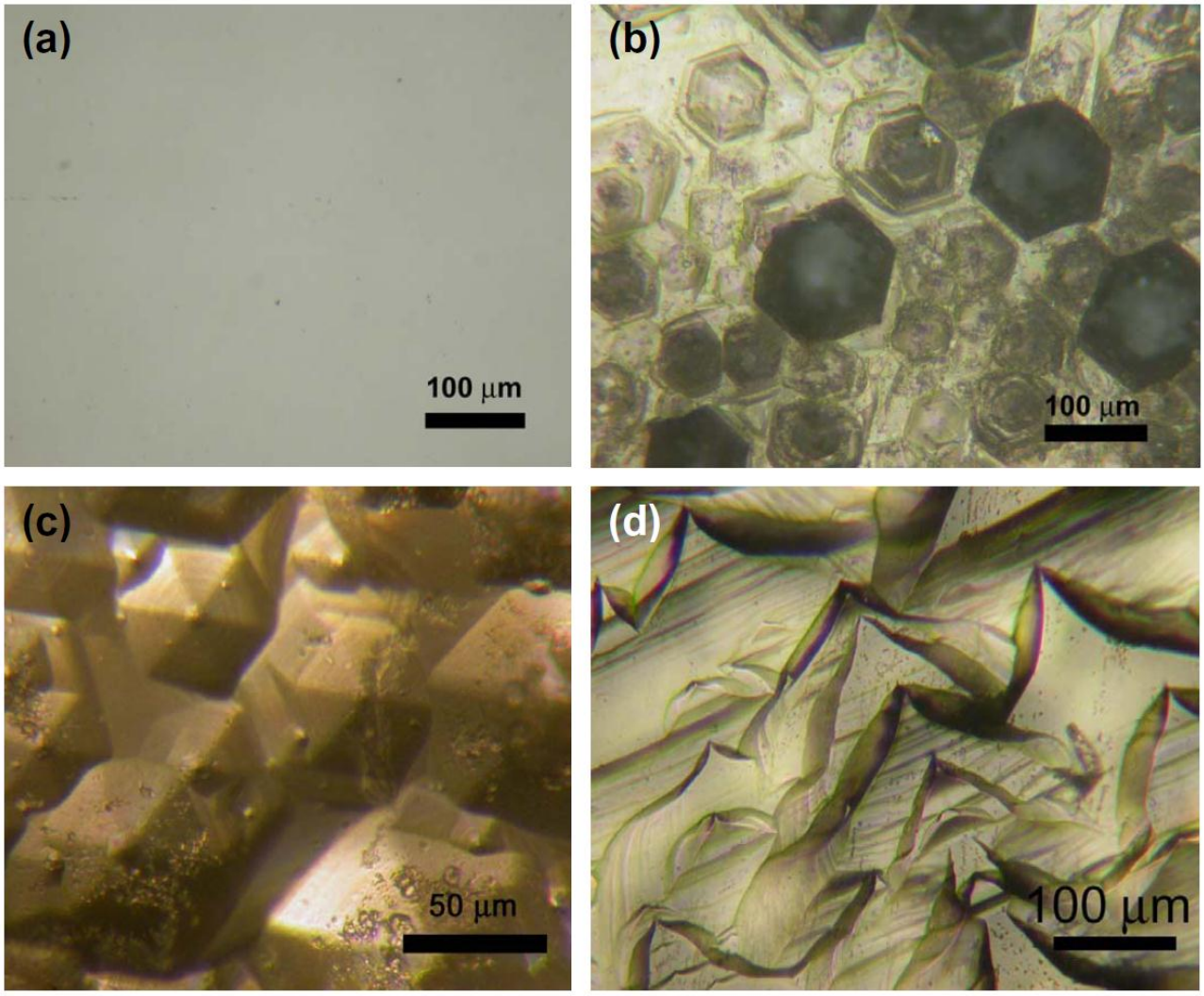

Figure 3 Light microscopy images of the surface of ZnO crystals: (a) virgin ZnO (0001) crystal; (b) hydrogen loaded ZnO (0001) crystal (t = 3h, I = 0.5 mA); (c) hydrogen loaded ZnO (0001) crystal illuminated by oblique light; (d) hydrogen loaded (t = 3h, I = 0.5 mA) ZnO (10-10) crystal.

Theoretical calculations performed in Ref. [5] revealed that hydrogen occupies bond-centered (BC) sites between O and Zn atoms and causes a significant outward relaxation of neighboring atoms. In the ZnO lattice one can distinguish two kinds of BC sites which differ by orientation of the O-H bond: (i) $BC_{\parallel}$ sites, where the O-H bond is parallel with the *c*-axis and (ii) $BC_{\perp}$ sites, where it is not parallel. Extended calculations with increased convergence and additional relaxation [16] indicated that the lowest energy sites are the $BC_{\parallel}$ positions, i.e. O-H bonds should be oriented predominantly in the *c*-direction. However, it has to be mentioned that the energy difference between the $BC_{\parallel}$ and $BC_{\perp}$ is very small (~ 0.1 eV). Hydrogen absorbed in ZnO and occupying $BC_{\parallel}$ sites causes a significant lattice expansion in the *c*-direction. Because of enhanced hydrogen concentration the hydrogen-induced lattice expansion in the sub-surface region is higher than in the rest of the crystal. Absorbed hydrogen introduces stress into the loaded crystal and when this stress

exceeds the ZnO yield stress plastic deformation of the crystal takes place and introduces open volume defects (dislocations and vacancies) into the sub-surface region. Excess hydrogen in the sub-surface region is trapped at these open volume defects introduced by plastic deformation. Trapped hydrogen atoms are immobile at room temperature and contribute to the enhanced hydrogen concentration detected in the sub-surface regions by NRA.

Hydrogen-induced plastic deformation causes a typical surface modification of ZnO crystals loaded with hydrogen. Light microscopy image of the surface of the virgin ZnO (0001) crystal is shown in Fig. 3(a). The virgin crystal exhibits obviously just a flat surface without any features. Fig. 3(b) shows light microscopy image of the surface of the ZnO (0001) crystal loaded with hydrogen using a current of 0.5 mA applied for a period of 3 h. One can see in the figure that a lot of hexagonally shaped pyramids were formed on the surface. Interestingly, all these pyramids have nearly the same orientation with respect to the crystal. Fig. 3(c) presents an image of the hydrogen loaded ZnO (0001) crystal taken in oblique light which confirms that the pyramids grow out of the crystal. This indicates that the pyramids were formed by hydrogen-induced plastic deformation realized by a slip in the *c*-direction. Surface modification of hydrogen loaded ZnO (10-10) crystal is shown in Fig. 3(d). Again hydrogen-induced slip took place in the *c*-direction which now lies in the plane of the surface. As a consequence, the pyramids are now rotated by 90^{o} with respect to Figs. 3(b,c), i.e. hydrogen-induced slip takes place in the surface plane.

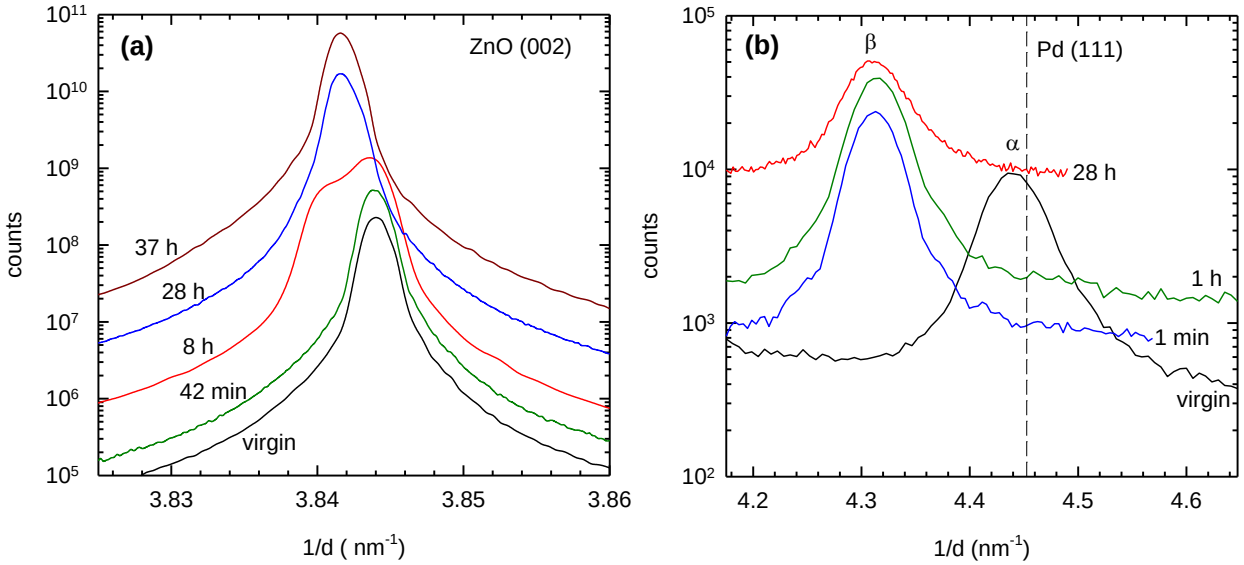

Figure 4 XRD results measured on ZnO (0001) crystal loaded with hydrogen (I = 0.5 mA) for various time periods: (a) the ZnO (002) reflection, (b) the Pd (111) reflection from the 20 nm thick Pd over-layer. Transformation of the Pd over-layer into the hydride phase (β) is clearly visible. Dashed line in the figure shows position of the (111) reflection in bulk Pd. For better clarity the XRD peaks for various loading periods were shifted in the vertical direction.

Results of XRD studies of ZnO (0001) crystal in the virgin state and electrochemically loaded with hydrogen using a current of 0.5 mA for various time periods are presented in Fig. 4. The ZnO (002) reflection is plotted in Fig. 4(a). Narrow width and very high intensity of this reflection testifies high quality of the ZnO crystal. Fig. 4(b) shows the Pd (111) reflection originating from the thin Pd over-layer. Obviously the Pd (111) reflection is rather broad due to nanocrystalline grain size and small thickness (20 nm) of Pd cap. The position of Pd (111) reflection in the virgin sample is close to that for bulk Pd indicating that stress induced by lattice mismatch between Pd over-layer and ZnO crystal is relatively low. During electrochemical charging hydrogen is firstly absorbed in Pd cap which undergoes a phase transition into the hydride β-phase (PdH). This phase transition leads to a shift of the (111) reflection to lower diffraction angles which is clearly visible in Fig. 4(b). Hydrogen loading for 1 min using the current of 0.5 mA is sufficient to transform Pd cap

completely into the hydride phase. During further hydrogen charging the Pd cap is kept in the hydride phase, which is testified by the Pd (111) reflection remaining at the position corresponding to the β-phase, and hydrogen from the Pd layer penetrates into ZnO and is absorbed there.

One can see in Fig. 4(a) that hydrogen loading leads firstly to a shift of the ZnO (002) reflection to lower diffraction angles due lattice expansion caused by absorbed hydrogen. In the crystal loaded further for 9 h the ZnO (002) reflection is split into two parts. Obviously this is due to formation of sub-surface region with enhanced hydrogen concentration which was detected by NRA. The ZnO (002) reflection in the sample loaded for 9 h is a superposition of diffraction from the sub-surface region containing very high hydrogen concentration and diffraction from deeper regions in ZnO crystal where the hydrogen concentration is lower. With increasing loading period the hydrogen enhanced sub-surface region extends more and more into the ZnO crystal and its thickness becomes higher than penetration depth of the X-rays. As a consequence, the ZnO (002) profile in the sample loaded for 28 h or longer period contains only the contribution from the sub-surface region.

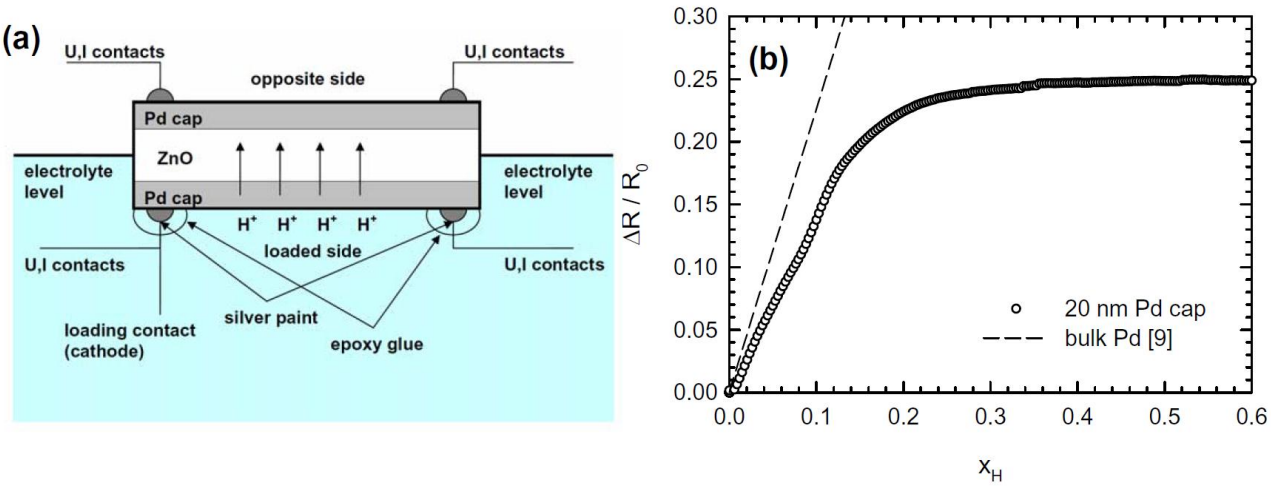

Figure 5 (a) Schematic depiction of the arrangement used in *in-situ* electrical resistivity measurements, (b) the relative increase of the electrical resistivity of Pd cap measured on the loaded side on ZnO (0001) crystal electrochemically charged with hydrogen using low current of 0.01 mA. Dashed line shows the relative increase of electrical resistivity for a bulk Pd [17].

The *in-situ* electrical resistivity measurement of hydrogen loaded ZnO crystals was performed in the configuration shown in Fig. 5(a). Both the loaded side and the opposite side were covered by 20 nm Pd cap. The loaded side was deluged by electrolyte while the opposite side was on air without any contact with the electrolyte. This configuration enables to measure resistivity independently on the loaded side and also on the opposite side. During hydrogen loading the Pd cap on the loaded side is firstly hydrogenated and transformed into the hydride phase. This process was firstly investigated in ZnO crystal loaded with low current of 0.01 mA and measured on the loaded side. Fig. 5(b) shows relative increase of electrical resistivity of the Pd cap as a function of the hydrogen concentration in Pd layer calculated by Eq. (1) under assumption that all hydrogen introduced into the sample remains in Pd cap. The electrical resistivity in Fig. 5(b) increases due to transformation of Pd layer into the hydride phase. The dashed line in Fig. 5(b) shows resistivity increment predicted by Geerken et al. [17] for a single phase interstitial solid solution of hydrogen in bulk Pd. Compared to bulk Pd the resistivity increment for Pd cap is lower due to hydrogen trapping at defects. This is typical behavior for nanocrystalline Pd films [18]. Complete transformation of the Pd cap into the hydride phase causes relative increase of resistivity $\Delta R/R_0 \approx 0.25$, which is in reasonable agreement with the values determined in Ref. [18] for very thin Pd films deposited on Si substrate.

In our previous work [12] we found that hydrogen diffusion in ZnO in the *c*-direction is rather fast and comparable with hydrogen diffusion in Pd. It is believed that this is due to open channels existing along the *c*-axis in the ZnO wurtzite structure and providing pathways for fast hydrogen

motion. In this work, we performed *in-situ* electrical resistivity studies of ZnO (0001) (*c*-orientation) and ZnO (10-10) (*a*-orietantion) crystal in order to examine possible anisotropy of hydrogen diffusion in ZnO. Fig. 6 shows the relative change of electrical resistivity $\Delta R/R_0$ measured on the loaded side and on the opposite side in *c*-oriented and *a*-oriented ZnO crystal. Both crystals have the same thickness of 0.5 mm and were loaded using the current of 0.1 mA. Behavior of the electrical resistivity measured on the loaded side is very similar in both crystals: the Pd layer is firstly hydrogenated and transforms into hydride phase (PdH) which is reflected by an increase of resistivity. A continuous flux of incoming hydrogen during further loading keeps the Pd cap in the hydride phase (i.e. its electrical resistivity remains approximately constant) and hydrogen penetrates into the ZnO crystal. Additional increase of electrical resistivity accompanied with increased scatter of resistivity data occurs at longer loading times (t > 2000 s), see Fig. 6. This is due to hydrogen-induced plastic deformation taking place in ZnO sub-surface layer and causing local destruction of Pd cap [12]. On the opposite side, the rise of electrical resistivity is postponed and occurs after an extended loading period of ≈ 14000 s in the *c*-oriented crystal and after an even longer period of ≈ 33000 s in the *a*-oriented crystal, see Fig. 6. The postponed response of the electrical resistivity on the opposite side is due to diffusion of hydrogen from the loaded side across the sample thickness towards the opposite side. Hence, the room temperature hydrogen diffusion coefficient D_H in ZnO crystal can be estimated from the time lag t_{lag} between the resistivity response on the loaded side and on the opposite side:

$$D_H \approx d^2 / 6\, t_{lag} \,. \qquad (2)$$

From Eq. (2) we obtained $D_H = (3.0 \pm 1.0) \times 10^{-12}$ m^{2}s^{-1} for the *c*-oriented crystal and $D_H = (1.3 \pm 0.6) \times 10^{-12}$ m^{2}s^{-1} for the ZnO crystal with *a*-orientation. This result testifies that hydrogen diffusion in ZnO in the *c*-direction [0001] is significantly faster than in the *a*-direction [10-10]. Anisotropy of hydrogen diffusion in ZnO is most probably due to open channels exiting in the ZnO wurtzite structure along the *c*-axis which facilitates hydrogen diffusion in the [0001] direction.

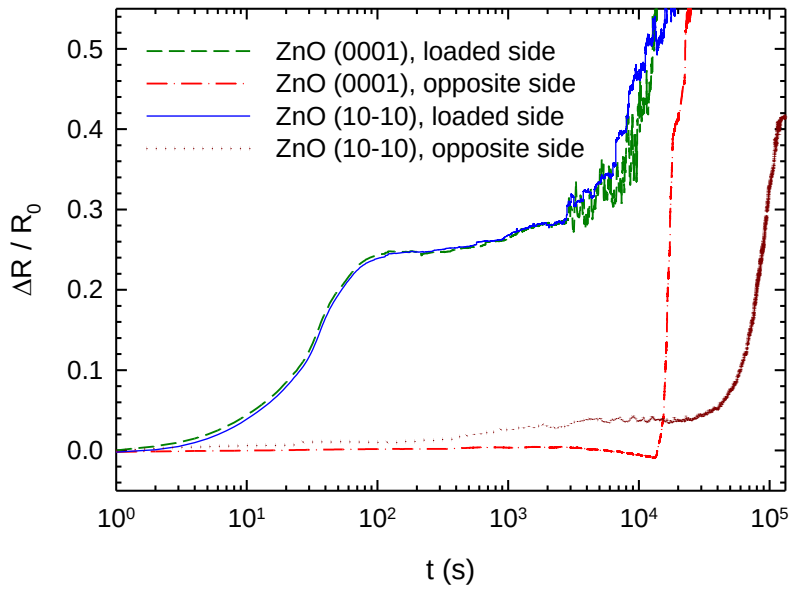

Figure 6 The relative increase of electrical resistivity in ZnO crystals with (0001) and (10-10) orientation loaded with hydrogen using the current of 0.5 mA. The samples were loaded in the arrangement shown in Fig. 5(a) and electrical resistivity was measured simultaneously on the loaded side and also on the opposite side

Summary

Hydrogen-induced structural changes and hydrogen diffusivity in ZnO crystals electrochemically loaded with hydrogen were studied. NRA characterization of hydrogen loaded crystals revealed that bulk hydrogen concentration introduced into the crystal agrees with the value calculated from Faraday's law. A sub-surface layer with significantly higher concentration of hydrogen is formed on the loaded side and also on the opposite side if it is in contact with electrolyte. SPIS characterizations revealed that hydrogen-induced plastic deformation introduces a high concentration of defects into the sub-surface regions. Hydrogen-induced slip in the *c*-direction causes a specific surface modification of ZnO crystals which was observed by light microscope. Using *in-situ* electrical resistometry the hydrogen diffusion coefficient in ZnO was determined. Hydrogen diffusion in the *c*-direction is faster than in the *a*-direction due to open channels existing in the ZnO wurtzite structure along the *c*-axis and facilitating hydrogen diffusion.

Acknowledgements

This work was supported by the Czech Science Foundation (project P108/11/0958) the Ministry of Education, Youths and Sports of the Czech Republic (projects MEB101102 and LH12173), the Charles University in Prague (project SVV-2012-265303) and the German Academic Exchange Service (project 71 31 308 022).

References

[1] D.C. Look, Mater. Sci. Eng. B Vol. 80 (2001), p. 383

[2] Ü. Özgür, Ya. I. Alivov, C. Liu, A. Teke, M. A. Reshchikov, S. Doğan, V. Avrutin, S.-J. Cho, and H. Morkoç, J. Appl. Phys. Vol. 98 (2005), p. 041301

[3] S.J. Pearton, D.P. Norton, K. Ip, Y.W. Heo, T. Steiner, Prog. Mater. Sci. Vol. 50 (2005), p. 293

[4] M.D. McCluskey and J. Jokela, J. Appl. Phys. Vol. 106 (2009), p. 071101

[5] C. G. Van de Walle, Phys. Rev. Lett. Vol. 85 (2000), p. 101233

[6] G. Brauer, W. Anwand, D. Grambole, J. Genzer, W. Skorupa, J. Čížek, J. Kuriplach, I. Procházka, C.C. Ling, C.K. So, D. Schultz and D. Klimm, Phys. Rev. B Vol. 79 (2009), p. 115212

[7] J. Čížek, N. Žaludová, M. Vlach, S. Daniš, J. Kuriplach, I. Procházka, G. Brauer, W. Anwand, D. Grambole, W. Skorupa, R. Gemma, R. Kirchheim and A. Pundt: J. Appl. Phys. Vol. 103 (2008), p. 053508

[8] P.J. Schultz and K.G. Lynn, Rev. Mod. Phys. Vol. 60 (1988), p. 701

[9] W.A. Lanford, in: Handbook of Modern Ion Beam Materials Analysis, edited by R. Tesmer and M. Nastasi, Materials Research Society, Pittsburg (1995), p. 193

[10] R. Kircheim, Prog. Mater. Sci. Vol. 32 (1988), p. 261

[11] W. Anwand, H.R. Kissener and G. Brauer, Acta Physica Polonica A Vol. 88 (1995), p. 7

[12] J. Čížek, F. Lukáč, M. Vlček, I. Procházka, F. Traeger, D. Rogalla, H.-W. Becker: Defect and Diffusion Forum Vols. 326-328 (2012), p. 459

[13] A.van Veen, H. Schut, M. Clement, J. de Nijs, A. Kruseman and M. Ijpma, Appl. Surf. Sci. Vol. 85 (1995), p. 216

[14] T. Koida, A. Uedono, A. Tsukazaki, T. Sota, M. Kawasaki and S.F. Chichibu, phys. stat. sol. (a) Vol. 201 (2004), p. 2841

[15] R. Krause-Rehberg and H.S. Leipner, Positron Annihilation in Semiconductors – Defect Studies, Springer, Berlin (1999)

[16] E. V. Lavrov, J. Weber, F. Börrnert, C. G. Van de Walle, and R. Helbig, Phys. Rev. B Vol. 66 (2002), p. 165205

[17] B. Geerken, R. Griessen: J. Phys. F, Metal Phys Vol. 13 (1983), p. 13

[18] S. Wagner, A. Pundt, Acta Mater. Vol. 58 (2010), p. 1387

Recent Advances in Mass Transport in Engineering Materials
10.4028/www.scientific.net/DDF.333

Anisotropy of Hydrogen Diffusivity in ZnO
10.4028/www.scientific.net/DDF.333.39